Eur. Phys. J. Special Topics **226**, 1739–1750 (2017)

DOI: 10.1140/epjst/e2017-70048-x

THE EUROPEAN PHYSICAL JOURNAL SPECIAL TOPICS

Regular Article

Parameter-dependent behaviour of periodic channels in a locus of boundary crisis

James Rankin[1,a] and Hinke M. Osinga[2,b]

[1] Department of Mathematics, University of Exeter, Harrison Building, North Park Road, Exeter EX4 4QF, UK
[2] Department of Mathematics, University of Auckland, Private Bag 92019, Auckland 1142, New Zealand

Received 10 February 2017 / Received in final form 27 March 2017
Published online 21 June 2017

Abstract. A boundary crisis occurs when a chaotic attractor outgrows its basin of attraction and suddenly disappears. As previously reported, the locus of a boundary crisis is organised by homo- or heteroclinic tangencies between the stable and unstable manifolds of saddle periodic orbits. In two parameters, such tangencies lead to curves, but the locus of boundary crisis along those curves exhibits gaps or channels, in which other non-chaotic attractors persist. These attractors are stable periodic orbits which themselves can undergo a cascade of period-doubling bifurcations culminating in multi-component chaotic attractors. The canonical diffeomorphic two-dimensional Hénon map exhibits such periodic channels, which are structured in a particular ordered way: each channel is bounded on one side by a saddle-node bifurcation and on the other by a period-doubling cascade to chaos; furthermore, all channels seem to have the same orientation, with the saddle-node bifurcation always on the same side. We investigate the locus of boundary crisis in the Ikeda map, which models the dynamics of energy levels in a laser ring cavity. We find that the Ikeda map features periodic channels with a richer and more general organisation than for the Hénon map. Using numerical continuation, we investigate how the periodic channels depend on a third parameter and characterise how they split into multiple channels with different properties.

1 Introduction

Boundary crisis was first studied in [27] as a new bifurcation for chaotic dynamical systems. It is mediated by a homo- or heteroclinic tangency between global stable and unstable manifolds of fixed points or periodic orbits and results in the sudden disappearance of a chaotic attractor as it touches the boundary of its own basin of

[a] e-mail: james.rankin@gmail.com
[b] e-mail: h.m.osinga@auckland.ac.nz

attraction. While the locus of homo- or heteroclinic tangency is generally a smooth curve in a two-parameter plane, the locus of boundary crisis is not smooth [6,16,17]. Indeed, the effect of a tangency between global (un)stable manifolds can be different, particularly when the attractor is not chaotic, and other phenomena may result, such as interior crisis, when a multi-component chaotic attractor merges into a larger chaotic attractor that consists of fewer or only one component [7], or basin boundary metamorphosis, where the basin boundary associated with the attractor changes from smooth to fractal [8,9]. Gallas, Grebogi and Yorke [6] discussed how the nature of the crisis bifucation along a two-parameter tangency locus changes at a so-called double-crisis vertex, where another curve of homoclinic or heteroclinic tangencies between manifolds of a different periodic orbit intersects. In [16,17], it was shown that the nature of the crisis bifurcation on a tangency locus also changes at points where the tangency locus crosses a curve of saddle-node bifurcations. The intersecting curve of saddle-node bifurcations gives rise to a periodic channel that constitutes an actual gap in the locus of boundary crisis. Periodic channels are the two-parameter versions of the well-known periodic windows in one-parameter bifurcation diagrams of systems with chaotic attractors such as the logistic map [3] or the Hénon map [10,23]. Hence, one should expect that there may be infinitely many periodic channels, which means that we cannot speak of a *curve* of boundary crisis bifurcation.

Despite the fact that boundary crisis is not a robust phenomenon in a two-parameter setting, numerical brute-force iterative methods and actual physical experiments will still highlight its existence [1,14,21,22,28]. The gaps in the locus of boundary crisis will typically only be visible at increasingly finer scales of parameter variations [6,16,17]. However, the basin of attraction of the attractor that exists in such a periodic window may be quite large. Hence, particularly in the study of boundary crisis, where the attractor is supposed to disappear, the periodic channels can be very important in determining parameter regimes that can be regarded as safe. Therefore, it is of interest to study the organisation of periodic channels and how they depend on parameters.

Periodic windows and, therefore, periodic channels in the Hénon map [10,23] are structured in a special way: The two-parameter channel arises from a curve SN_k of saddle-node bifurcations that creates a saddle and sink of a particular period k; this is the base period of the channel. The period-k sink subsequently undergoes a cascade of period-doubling bifurcations until a chaotic attractor emerges that consists of k disjoint components. The basin of this chaotic attractor is formed by the stable manifold of the period-k saddle, and one branch of its unstable manifold accumulates onto the period-k attractor. The channel ends when the stable and unstable manifolds of the period-k saddle become tangent; this can give rise to an interior crisis after which the original chaotic attractor re-emerges, or a boundary crisis that destroys the k-component chaotic attractor. Using terminology from [7], we call this a periodic channel of subduction-crisis type. All periodic channels for the Hénon map are of subduction-crisis type and the order in which the sequence of bifurcations occurs is always the same, that is, if the left boundary for one of the periodic channels is formed by a curve of saddle-node bifurcation, then all left boundaries of the periodic channels are saddle-node bifurcations [16,17].

In this paper we investigate parameter dependence of periodic channels for the particular example of the Ikeda map [12,13]. This map describes the behaviour of the complex-field amplitude of a continuous laser signal as it recirculates through a dielectric nonlinear medium in a ring cavity, which is formed by four reflective mirrors. Light with constant amplitude and frequency is injected by the laser into the ring cavity and some of the energy is absorbed by the nonlinear medium. We use a simplified model of this process, which is derived in [11] by assuming that saturable absorption

is negligible; in real form, the Ikeda map is then given by the diffeomorphism

$$\begin{pmatrix} x \\ y \end{pmatrix} \mapsto \begin{pmatrix} a \\ 0 \end{pmatrix} + R \begin{pmatrix} \cos\vartheta & -\sin\vartheta \\ \sin\vartheta & \cos\vartheta \end{pmatrix} \begin{pmatrix} x \\ y \end{pmatrix}, \quad \text{where } \vartheta = \phi - \frac{p}{1+x^2+y^2}. \tag{1}$$

We view a and $0 \leq R \leq 1$ as the main parameters, which represent the amplitude of the light from the laser and the scaled reflectivity of the mirrors, respectively. The parameters ϕ and p are detuning parameters due to the cavity and nonlinear medium, respectively. In certain parameter regimes, the Ikeda map exhibits a chaotic attractor that coexists with a stable fixed point. The basic bifurcation structure that creates the chaotic attractor is a period-doubling sequence to chaos. The chaotic attractor is destroyed by a homoclinic tangency bifurcation between the global stable and unstable manifolds of the saddle fixed point, or a heteroclinic tangency bifurcation between the global stable and unstable manifolds of two saddle periodic orbits with periods six and two, respectively [6]. However, as was also already reported in [6], the precise region of existence of the chaotic attractor is more complicated due to the existence of many periodic channels, which also protrude into the regime where the stable fixed point is the only attractor.

We studied periodic channels for the Ikeda map (1) in detail in [19], where we kept $\phi = 0.4$ and $p = 6.0$ fixed. We found that the periodic channels in the (a, R)-plane of the Ikeda map (1) are not necessarily of subduction-crisis type [19], which makes the overall structure of its crisis loci richer than that of the Hénon map. In [19], we found periodic channels bounded on both sides by curves of saddle-node bifurcation, which we call subduction-subduction channels. Furthermore, there exist pairs of subduction-crisis channels of the same base period for which the ordering of the bifurcations in one of the channels occurs in a reversed 'crisis-subduction' manner. Both types of channels seem related to the so-called bounded or paired cascades of period-doubling bifurcations discussed in [24,25], which are created or destroyed in pairs that correspond to the same base period. Most importantly, as shown in [24], bounded cascades are not robust.

Our hypothesis is that variation of a third parameter for the Ikeda map will, therefore, cause the creation or destruction of periodic channels, namely, those of subduction-subduction or paired subduction-crisis type. In this paper, we use ϕ as this third parameter and study how the organisation of crisis loci and periodic channels in the (a, R)-plane changes as ϕ decreases. Here, we focus on periodic channels with base period five, which provide a good overview of the possible cases that can be expected. Since the creation and destruction of the period-doubling cascades is already discussed at length in [24,25], we are primarily interested in the effective splitting of a channel, caused by the creation of an additional locus of boundary crisis.

We complement the brute-force iteration methods that identify the loci of boundary crisis for the Ikeda map (1) in the (a, R)-plane with continuation methods that compute the loci of saddle-node and period-doubling bifurcation, as well as loci of homoclinic or heteroclinic tangencies between global stable and unstable manifolds of fixed points or periodic orbits. These loci were computed with the continuation package CL_MATCONT [4].

The presentation is organised as follows. In the next section, we present the local bifurcation structure near the period-five channels in the (a, R)-plane for four different values of ϕ. We describe the nature of the period-five channels and show how they depend on ϕ. In Section 3, we investigate how the locus of boundary crisis is involved in the splitting of a period-five channel. We end with a discussion in Section 4.

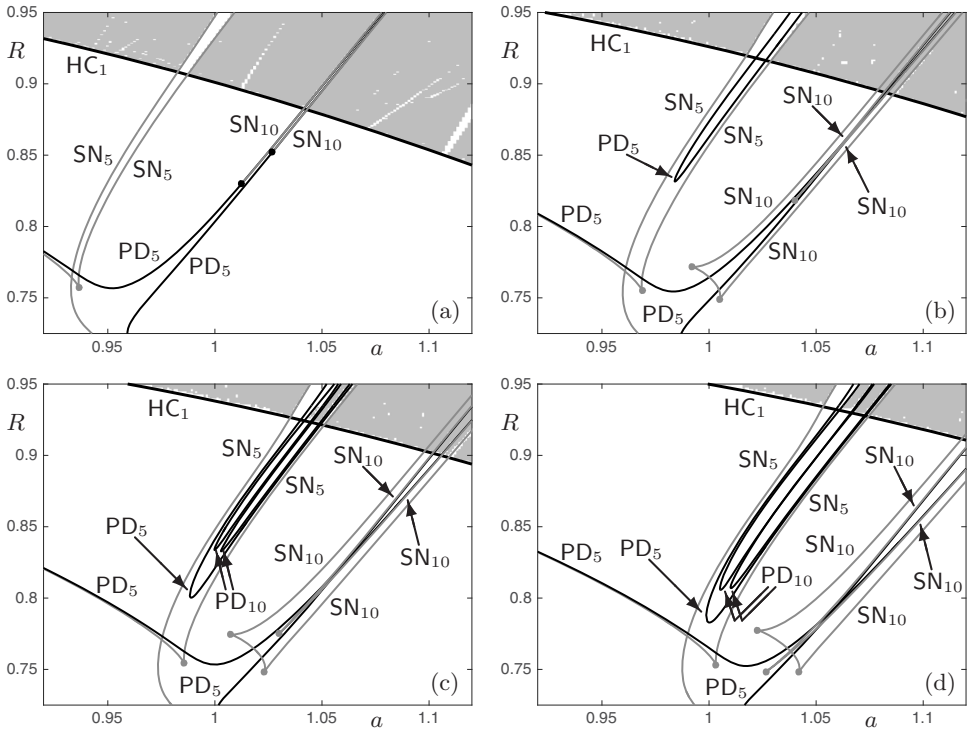

Fig. 1. Loci of saddle-node (grey) and period-doubling bifurcation (black) in the (a, R)-plane for the Ikeda map (1) with $p = 6.0$; the detuning ϕ decreases from $\phi = 0.4$, $\phi = 0.3$, $\phi = 0.25$ to $\phi = 0.2$ in panels (a)–(d), respectively. In the grey region, the only attractor is a stable fixed point; this region is bounded, in part, by the curve HC_1 (thick black) of homoclinic tangency between the stable and unstable manifolds of a saddle fixed point. Also indicated are curves SN_5 and SN_{10} of saddle-node bifurcation and PD_5 and PD_{10} of period-doubling bifurcation with base periods five and ten, respectively. The grey and black dots are cusp points and degenerate period-doubling points, respectively.

2 Parameter-dependence of period-five channels

Under normal operating conditions, the dynamics of the laser ring cavity is trivial, that is, the Ikeda map (1) has a single attractor that is a fixed point corresponding to coherent light of fixed complex-field amplitude. However, if the amplitude $a > 0$ of the incoming light is small enough and the reflectivity $0 \leq R \leq 1$ of the mirrors large enough, then other behaviour may occur, including chaos [5]. Figure 1 shows a small part of this region that focusses on the period-five channels in the (a, R)-plane. Here $p = 6.0$ is fixed, but ϕ is varied from $\phi = 0.4$, $\phi = 0.3$, $\phi = 0.25$ to $\phi = 0.2$ in panels (a)–(d), respectively. The grey-shaded regions correspond to parameter values for which the fixed point is the only attractor. For other parameter values, a second attractor co-exists, which may be chaotic. The lower boundary of the region with trivial dynamics is primarily formed by a locus HC_1 of homoclinic tangency between the stable and unstable manifolds of a saddle fixed point. Where HC_1 is indeed bounding the region of trivial dynamics, the homoclinic tangency bifurcation corresponds to a boundary crisis at which the chaotic attractor, which consists of a single component, suddenly disappears. The grey region of trivial dynamics is interspersed by periodic channels, several of which can easily be discerned, particularly in Figure 1a.

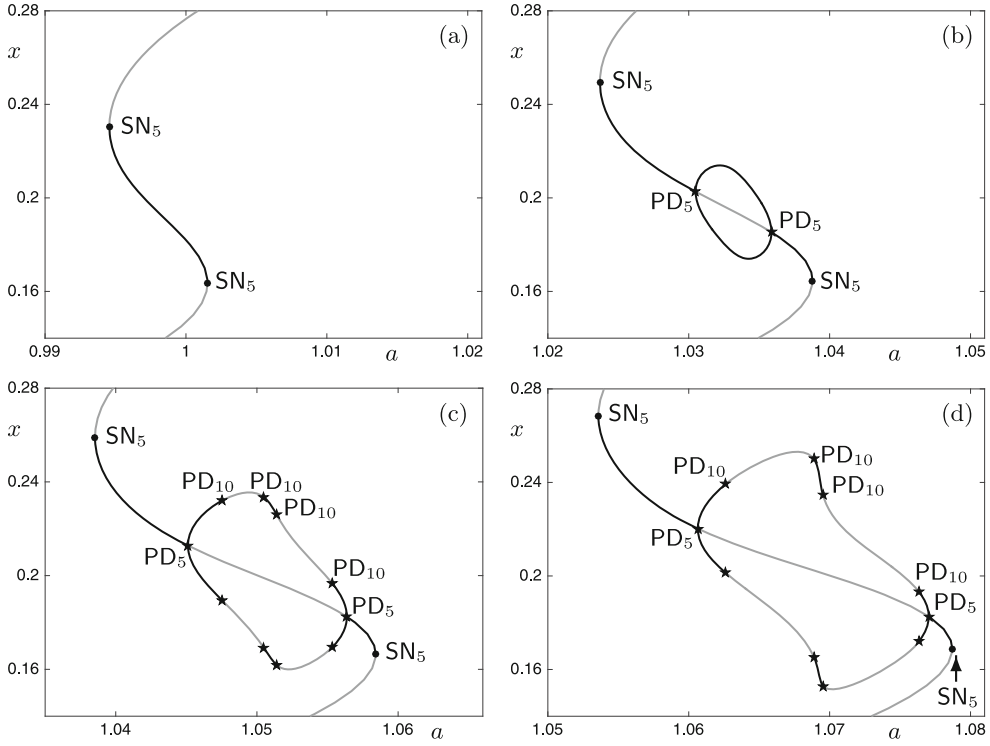

Fig. 2. Bifurcation diagram of the period-five base orbit for $R = 0.935$ and the same values $\phi = 0.4$, $\phi = 0.3$, $\phi = 0.25$ and $\phi = 0.2$ in panels (a)–(d) as in Figure 1, respectively. In each panel, a varies over a range that includes the width of the left period-five channel in the corresponding panels of Figure 1. The value of x of only one of the points in the period-five orbit is shown on the vertical axis, and two points are shown if the orbit has period ten. Stable solutions are black and unstable solutions are grey; the bifurcations are labelled as in Figure 1 with saddle-node and period-doubling points marked as dots and stars, respectively.

Two of these periodic channels have base period five and associated curves SN_5 and SN_{10} of saddle-node bifurcation and PD_5 and PD_{10} of period-doubling bifurcation of the period-five and -ten orbits in these channels are drawn and labelled as well; see also Figure 4, which shows a higher-resolution computation of the finer detail close to these channels in the parameter regime above HC_1.

Previous work investigating the organisation of solutions in the (a, R)-plane have used $\phi = 0.4$ and the data shown in Figure 1a was previously discussed in [19]. Let us first focus our attention on the left period-five channel, which is of subduction-subduction type and bounded on both sides by curves SN_5 of saddle-node bifurcation of a period-five orbit. Figure 2a shows a bifurcation diagram with respect to a, where R is fixed at $R = 0.935$, cutting across this channel at a location above the curve HC_1 associated with the locus of boundary crisis. Here, each period-five orbit is indicated by the x-coordinate of only one of its points. At either extreme of the a-range shown in Figure 2a, the trivial fixed point (not shown) is the only attractor that co-exists with a single saddle period-five orbit (grey). These period-five saddles are connected via a branch of stable period-five orbits (black) arising through a pair of saddle-node bifurcations SN_5. Above HC_1 the period-five channels represents an isolated region in the (a, R)-plane for which a stable period-five orbit exists; just below HC_1, the channel

forms a periodic window for the main chaotic attractor. For values of R well below HC_1, a cusp point exists on SN_5 and the general nature of the channel boundaries change; further bifurcations that produce higher-period attractors exist in this region, which we do not discuss further.

Figure 1b shows a similar bifurcation structure for $\phi = 0.3$. Note that the curve HC_1 has moved up and right, and the curves SN_5 are further apart. The wider period-five channel on the left contains what we will call a *finger*, bounded by a curve PD_5 of period-doubling bifurcation. The corresponding bifurcation diagram along the line $R = 0.935$ is shown in Figure 2b. There now exists a pair of period-doubling bifurcations PD_5 of the stable period-five orbit that give rise to a branch of stable period-ten orbits; the two points on the period-ten orbit that merge with the point used to indicate the period-five orbit are shown in Figure 2b. The finger inside the period-five channel extends down as far as $R \approx 0.83$. Below this minimum value of R, though well above the cusp point on SN_5, any cross-section of the channel is like that of Figure 2a.

The bifurcation structure increases in complexity as ϕ is decreased further. Panels (c) and (d) of Figure 1 show the situation for $\phi = 0.25$ and $\phi = 0.2$, where two additional fingers have appeared inside the finger bounded by PD_5. The two new fingers are bounded by curves PD_{10} of period-doubling bifurcation, meaning that the period-five channel now also contains regions where an attracting period-twenty orbit exists. The corresponding slices at $R = 0.935$ are shown in Figures 2c and 2d, respectively. Only periodic orbits with periods five and ten are plotted, along with the pair SN_5 of saddle-node bifurcations and the first two period-doubling bifurcations. For both ϕ-values further period-doubling bifurcations occur, though we suspect that the sequence is still finite for $\phi = 0.25$. The discerning eye will have spotted the grey-shaded regions above HC_1 inside the fingers bounded by PD_{10} in Figures 1c and 1d, which indicate that, for $R > 0.935$ large enough the period-doubling sequence is infinite and a chaotic attractor consisting of five components co-exists with the attracting fixed point in certain regions of the (a, R)-parameter plane.

The bifurcations inside the period-five channel as ϕ decreases is entirely in line with the findings reported by Sander and Yorke [24,25]. The boundary curves SN_5 correspond to the beginning and end of a paired cascade that includes increasingly more period-doubling bifurcations as ϕ decreases. The higher-order nonlinearities of the Ikeda map (1) cause the appearance of two instead of one finger that corresponds with the second period-doubling PD_{10}, which means that the paired cascade with base period five now includes a split of two paired cascades with base period ten; see also [25].

The second period-five channel in Figure 1 is also of subduction-subduction type. This channel exhibits the splitting and merging of a different type of paired cascade that is also discussed in [24,25]. Figure 3a1 shows a cross-section for $R = 0.935$ and $\phi = 0.4$, when the channel has its simplest form. Above the curve HC_1, it is bounded on both sides by curves SN_{10} of saddle-node bifurcation of a period-ten orbit that subsequently bifurcates to the base period-five orbit in a pair of (reversed) period-doubling bifurcations PD_5 [19]. As indicated in Figure 1a, the curves SN_{10} end on PD_5 at degenerate period-doubling bifurcation points, where the criticality of the period-doubling changes from supercritical to subcritical. This is illustrated in Figure 3a2 with a cross-section at $R = 0.82$ for this same ϕ-value; here, both period-doubling bifurcations PD_5 are subcritical.

As ϕ decreases, a cusp point gives rise to a pair of saddle-node bifurcations SN_5 on the middle branch of stable period-five orbits. Figures 3b1 and 3b2 show the same two cross-sections for $\phi = 0.3$, that is, at $R = 0.935$ and $R = 0.82$, respectively. For $\phi = 0.3$, there are additional period-doubling bifurcations PD_{10} for the branch of period-ten orbits that emanates from PD_5; each branch exhibits one period-doubling

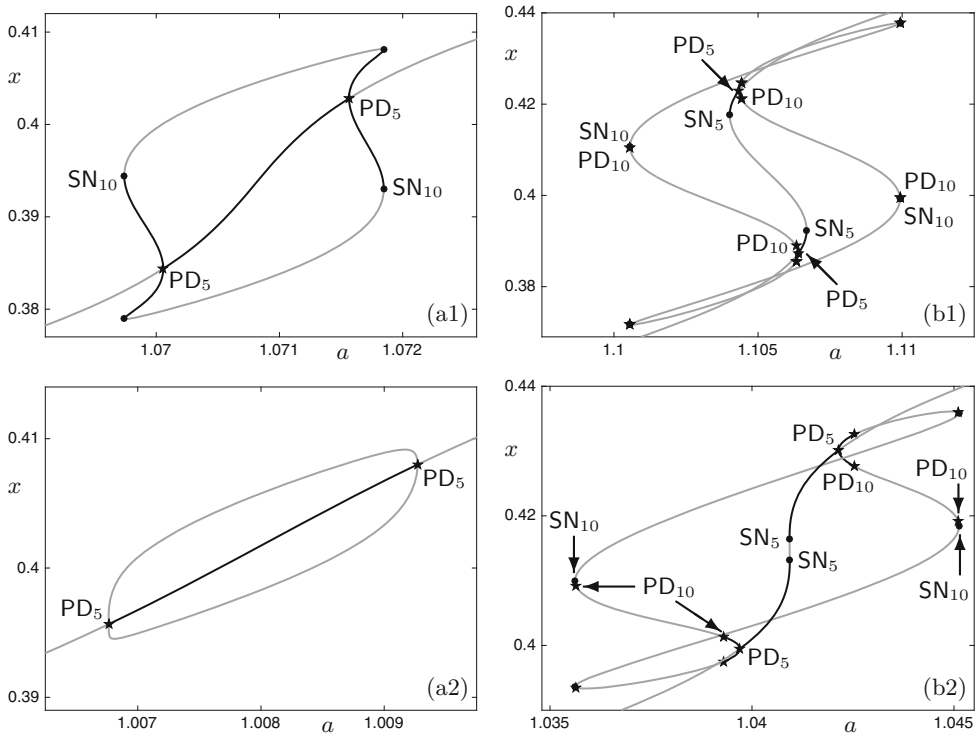

Fig. 3. Bifurcation diagram of the period-five base orbit for cross-sections $R = 0.935$ and $R = 0.82$ in rows 1 and 2, respectively. Panels (a1) and (a2) are for $\phi = 0.4$ and panels (b1) and (b2) for $\phi = 0.3$. In each panel, a varies over a range that includes the width of the right period-five channel in Figures 1a or 1b. The value of x of only one of the points in the period-five orbit is shown on the vertical axis, and two points are shown if the orbit has period ten. Stable solutions are black and unstable solutions are grey; the bifurcations are labelled as in Figure 1 with saddle-node and period-doubling points marked as dots and stars, respectively.

bifurcation soon after PD_5 and a second (backward) one just before the saddle-node bifurcation SN_{10}, indicating the existence of two paired cascades with base period ten, each in between SN_{10} on one side and PD_5 on the other. These paired cascades each generate two separate subduction-crisis channels; we note that the channels close to SN_{10} are narrow in a. We observe from Figure 1b that the two curves PD_5 of period-doubling bifurcations cross as R increases, which can be seen more clearly in panels (c) and (d), where $\phi = 0.25$ and $\phi = 0.2$, respectively. Another way to look at this is that, for fixed R, two channels change places in a as ϕ decreases and the curves SN_5 move further apart. Indeed, as shown in Figure 3b1 for $R = 0.935$ and $\phi = 0.3$, the boundaries for the period-five channels are saddle-node bifurcations SN_5, and the other boundaries are given by the limits of infinite period-doubling cascades; we only show the first two period-doubling bifurcations PD_5 and PD_{10}. Similarly, the channels with base period ten are bounded on one side by SN_{10} and on the other by infinite cascades over narrow ranges in a. The cross-section for $R = 0.82$ and $\phi = 0.3$ in Figure 3b2 is qualitatively the same as for $R = 0.935$ in panel (b1), but the two saddle-node bifurcations SN_5 are very close together, indicating the presence of a cusp point for slightly smaller value of R; this cusp point lies at $R \approx 0.819$ and is shown in Figure 1b.

3 Channel splitting due to boundary crisis

The period-five channels discussed in Section 2 are parameter-dependent versions of paired cascades. The depth of the cascade may vary with ϕ, and the complexity increases as ϕ decreases. As soon as ϕ is small enough and the paired cascade is complete, in the sense that it contains an infinite sequence of period-doubling bifurcations with the limiting chaotic attractor, we may observe a splitting of the channel for parameter values at which the chaotic attractor exhibits a boundary crisis. We observe this phenomenon in Figure 1. For example, the grey shading in panel (d) inside the fingers bounded by PD_{10} of the left period-five channel indicates that the chaotic attractor created in the period-doubling cascade has disappeared. The period-five channel has split into (at least) two channels: both are of classic subduction-crisis or (the reverse) crisis-subduction type, with the left-most channel being the widest and clearly showing the expected order of SN_5 followed by PD_5 and PD_{10}, indicating the existence of a homoclinic tangency HC_5 between the (un)stable manifolds of the saddle periodic orbit created in SN_5 that bounds the channel on the right-hand side.

Figures 1b–1d illustrate that the fingers bounded by period-doubling bifurcations are oriented such that their tips point towards decreasing R, which means that the complexity or depth of the cascade is increasing as R increases, at least when ϕ is small enough. Since the complexity of the paired cascade is 'added at the top' one might conclude that the channel splitting then also originates at, say, $R > 0.95$ in the (a, R)-plane. We find that, in fact, the exact opposite occurs.

The mechanism that splits a channel is illustrated in Figure 4 with a closer inspection of the first (left-hand) period-five channel in the (a, R)-plane for each of the ϕ-values in Figure 1; the ranges for a and R vary in these panels, sometimes beyond that of Figure 1. The grey shading for these enlargements is computed at a higher resolution, but particularly stubborn transients persist in the region just above HC_1 and near the curves SN_5 and PD_{10}, even after 10^7 iterates; similarly, some anomalous shading appears inside a white region, indicating that the co-existing attractor has an extremely small basin. We have chosen not to resolve these numerical issues in detail. The first two panels in Figure 4 are primarily for completeness, illustrating that the bifurcation structure near the homoclinic tangency HC_1 is, indeed, entirely explained by the slices for fixed $R = 0.935$ shown in Figures 2a and 2b, respectively. For $\phi = 0.4$ in Figure 4a, the period-five channel is bounded by the saddle-node bifurcation SN_5. The boundary remains unchanged for $\phi = 0.3$, but a finger bounded by period-doubling bifurcation PD_5 has appeared inside the channel; see Figure 4b.

The splitting of the period-five channel occurs in Figures 4c and 4d, corresponding to $\phi = 0.25$, and $\phi = 0.2$, respectively. At $\phi = 0.2$, the period-five channel has split into three channels. Note the classic subduction-crisis type of the left-most channel, including an infinite period-doubling cascade as indicated by the successive order, from left to right, of curves SN_5, PD_5, PD_{10}, ending in a boundary crisis. The left channel is paired with another (reversed) subduction-crisis channel with base period five on the right, and the third channel is of crisis-crisis type with base-period ten, located in between these two paired channels. Two period-doubling cascades, starting with PD_{10} lie within this crisis-crisis channel and face the flanking base-five cascades on each side.

The mechanism that brings about the splitting of the period-five channel is implied by the situation shown for $\phi = 0.25$ in Figure 4c, which illustrates a transitional phase. For large R, the channel has split into only two channels: the channel on the right exhibits the classic (reversed) subduction-crisis type with base period five, and the channel on the left exhibits this same cascade starting with SN_5, but interspersed with a paired cascade of base period ten on the period-doubled branch that starts and ends with PD_{10}; this paired cascade is not infinite when R is large, but for values

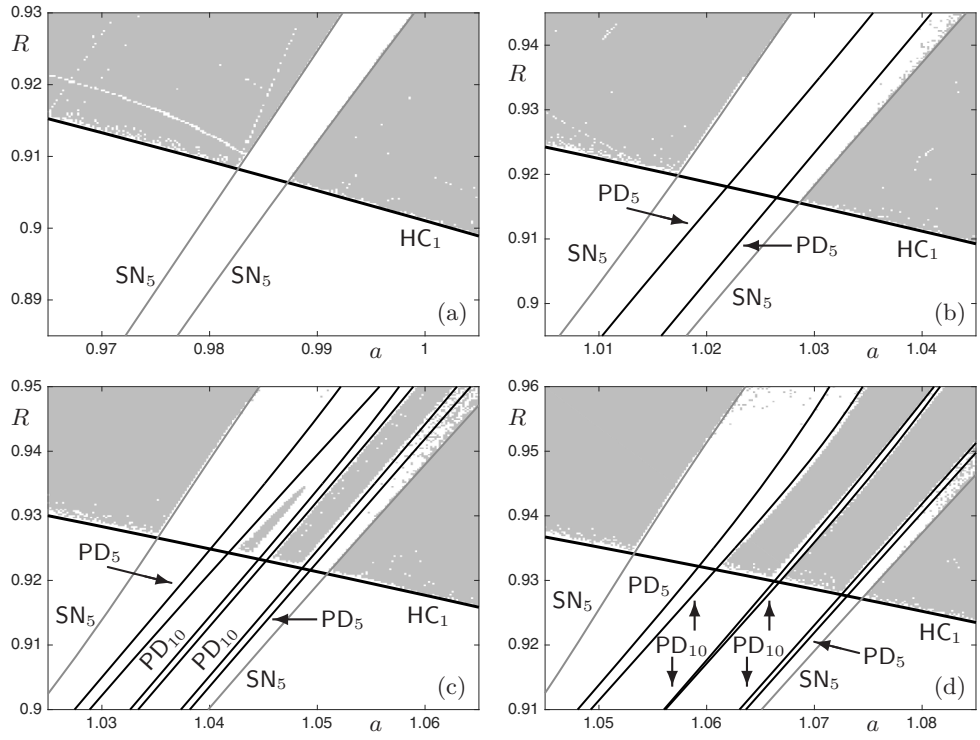

Fig. 4. Enlargements of the bifurcation diagram in the (a, R)-plane near the first period-five channel for the same values $\phi = 0.4$, $\phi = 0.3$, $\phi = 0.25$ and $\phi = 0.2$ in panels (a)–(d) as in Figure 1, respectively. As before, in the grey region, the only attractor is a stable fixed point; the loci SN_5 of saddle-node (grey), PD_5 and PD_{10} of period-doubling (black) and HC_1 of homoclinic tangency bifurcation (thick black) are labelled accordingly; see also Figure 1.

of R just above HC_1 it becomes a complete paired cascade, as indicated by the grey-shaded finger, or better, finger nail of trivial fixed-point dynamics that protrudes up with its tip pointing towards increasing R. As can be inferred from Figure 4, the tip of the finger moves up in R as ϕ decreases.

The paired cascade starting from SN_5 on either side of the original period-five channel is expected to complete with a homoclinic tangency between the stable and unstable manifolds of the co-existing saddle periodic orbit with the same base period of five. Unfortunately, while we could confirm the existence of this tangency HC_5, we have been unable to continue it as a curve in the (a, R)-plane; there is a numerical difficulty caused by the extreme stretching along the stable manifold. Figure 5 shows a sketch of the organisation in the (a, R)-plane near the grey-shaded finger nail of trivial fixed-point dynamics at $\phi = 0.25$. The entire finger is bounded by a curve HC_5 of homoclinic tangency bifurcation involving the global stable and unstable manifolds of the period-five saddle that originates from SN_5. The nail is created due to the intersection of HC_1 with HC_5. The boundary of the grey-shaded region corresponds to a boundary crisis, which involves a single-component chaotic attractor along HC_1 and a five-component chaotic attractor along HC_5. The intersection points, labelled $\mathsf{V}^{\pm}_{1,5}$, are double-crisis-vertices. In the direction of increasing a, the nature of the homoclinic tangency HC_1 changes at $\mathsf{V}^{+}_{1,5}$ from a basin boundary metamorphosis, where the basin boundary changes from being the stable manifold of a saddle fixed

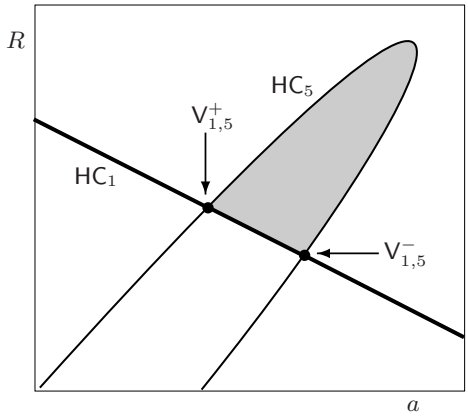

Fig. 5. Sketch of the organisation in the (a, R)-plane near the grey-shaded finger nail of trivial fixed-point dynamics inside one of the fingers bounded by PD_{10} for $\phi = 0.25$. The locus HC_1 is intersected by the parabola-shaped locus HC_5 of homoclinic tangency between (un)stable manifolds of a period-five saddle. The intersection points are two double-crisis vertices, labelled $\mathsf{V}^{\pm}_{1,5}$, that delimit a short segment along HC_1 that corresponds to a boundary crisis.

point to the stable manifold of the period-five saddle, to a boundary crisis; at $\mathsf{V}^{-}_{1,5}$, it changes back from a boundary crisis to a basin boundary metamorphosis. In the direction of increasing R, the nature of the homoclinic tangency HC_5 changes at $\mathsf{V}^{+}_{1,5}$ from an interior crisis to a boundary crisis, and the same occurs at $\mathsf{V}^{-}_{1,5}$.

Note that the appearance of the finger bounded by HC_5 occurs inside the finger bounded by PD_{10}, which points in the opposite direction; see Figure 1c. One could conclude that HC_5 must, therefore, have a minimum in the (a, R)-plane, which means that the finger is actually an oval bounded by a closed curve. However, the homoclinic tangency HC_5 is not constrained by the presence of a period-doubling bifurcation, which stipulates the nested nature of the curves PD_5 and PD_{10}. It is our hypothesis that HC_5 behaves similar to HC_1, that is, it consists of a single curve that connects this segment of HC_5 with the other two homoclinic tangeny bifurcations of the period-five saddle that enter or leave Figure 4c through the horizontal axes at $R = 0.95$ and $R = 0.9$. This means that HC_5 must intersect each of the curves PD_{10} and all other higher-period period-doubling curves, which would change the number of components of the chaotic attractor involved in the interior crisis along HC_5. The precise details of how this is organised are left for future work.

4 Discussion

We studied the nature and organisation for the Ikeda map (1) of periodic channels persisting in a parameter regime of predominantly trivial dynamics, where the main chaotic attractor has been destroyed in a boundary crisis. Due to the higher-order nonlinearity of the Ikeda map, these periodic channels are not as structured and ordered as for the Hénon map. Rather they arise from so-called paired cascades [24,25] associated with a particular base periodic orbit. The splitting of a channel occurs via the completion in a paired cascade of a period-doubling sequence to chaos, culminating in a homo- or heteroclinic tangency involving (one of) the manifolds of the base periodic orbit that occurs inside the channel; the tangency causes a boundary crisis of the chaotic attractor created in the period-doubling cascade.

We found the direction of variation in R that increases the complexity of the paired cascade to be precisely opposite from that which brings about the manifold tangency. Hence, as ϕ decreases, the channel splits from the inside with a finger or bubble of boundary crisis involving a chaotic attractor with a different number of components that protrudes from the main boundary crisis locus. Such bubbles have been observed before in a three-parameter study of a quasi-periodically forced Hénon map [18], but have not previously been observed in two-dimensional maps.

In future work, we hope to tackle the numerical challenge of continuing a homoclinic tangency associated with a period-five orbit that has a strongly contracting eigenvalue. It would also be of interest to identify bubbles associated with splitting of a periodic channel for other two-dimensional systems, and perhaps for a channel with a lower base period; we have checked the period-three channels for the Ikeda map, where such bubbles do not seem to exist [19]. A complete understanding of this kind of channel splitting for two-dimensional maps would certainly help in the investigation of similar behaviour for quasi-periodically forced or other higher-dimensional systems; for example, channel splitting may well play a role in the phenomena reported in [26, 29].

HMO is grateful to Ulrike Feudel for introducing her to boundary crisis more than 20 years ago. At the time, they tackled the harder problem of boundary crisis in quasi-periodically forced systems. Their discovery of the 'bubble' in the locus of boundary crisis for the quasi-periodically forced Hénon map, and a need to understand how such bubbles come about, has led to this paper. Happy birthday Ulrike!

References

1. N. Blackbeard, H. Erzgräber, S. Wieczorek, Shear-induced bifurcations and chaos in models of three coupled lasers, SIAM J. Appl. Dyn. Syst. **10**, 469 (2011)
2. J.-P. Carcassès, C. Mira, M. Bosch, C. Simó, J.C. Tatjer, Crossroad area-spring area transition I. Parameter plane representation, Int. J. Bifurc. Chaos **1**, 183 (1991)
3. R.L. Devaney, *An Introduction to Chaotic Dynamical Systems* (Addison-Wesley Publishing Company, Inc., 1987)
4. A. Dhooge, W. Govaerts, Y.A. Kuznetsov, W. Mestrom, A.M. Riet, Cl_matcont: a Continuation Toolbox in Matlab, in *Proceedings of the ACM Symposium on Applied Computing, 2003* (ACM New York, 2003), pp. 161–166
5. Z. Galias, Rigorous investigation of the Ikeda map by means of interval arithmetic, Nonlinearity **15**, 1759 (2002)
6. J.A. Gallas, C. Grebogi, J.A. Yorke, Vertices in parameter space: double crises which destroy chaotic attractors, Phys. Rev. Lett. **71**, 1359 (1993)
7. C. Grebogi, E. Ott, J.A. Yorke, Crises, sudden changes in chaotic attractors, and transient chaos, Physica D **7**, 181 (1983)
8. C. Grebogi, E. Ott, J.A. Yorke, Metamorphoses of basin boundaries in nonlinear dynamical systems, Phys. Rev. Lett. **56**, 1011 (1986)
9. C. Grebogi, E. Ott, J.A. Yorke, Basin boundary metamorphoses: Changes in accessible boundary orbits, Physica D **24**, 243 (1987)
10. M. Hénon, A two-dimensional mapping with a strange attractor, Comm. Math. Phys. **50**, 69 (1976)
11. S.M. Hammel, C.K.R.T. Jones, J.V. Moloney, Global dynamical behaviour of the optical field in a ring cavity, J. Opt. Soc. Amer. B **2**, 552 (1985)
12. K. Ikeda, Multiple-valued stationary state and its instability of the transmitted light by a ring cavity system, Opt. Comm. **30**, 257 (1979)
13. K. Ikeda, H. Daido, O. Akimoto, Optical turbulence: Chaotic behavior of transmitted light from a ring cavity, Phys. Rev. Lett. **45**, 709 (1980)

14. J.F. Mason, P.T. Piiroinen, Interactions between global and grazing bifurcations in an impacting system, Chaos **21**, 013113 (2011)
15. C. Mira, J.-P. Carcassès, M. Bosch, C. Simó, J.C. Tatjer, Crossroad area-spring area transition II. Foliated parametric representation, Int. J. Bifurc. Chaos **1**, 339 (1991)
16. H.M. Osinga, Locus of boundary crisis: Expect infinitely many gaps, Phys. Rev. E **74**, 035201(R) (2006)
17. H.M. Osinga, Boundary crisis bifurcation in two parameters, J. Diff. Eq. Appl. **12**, 997 (2006)
18. H.M. Osinga, U. Feudel, Boundary crisis in quasiperiodically forced systems, Physica D, **141**, 54 (2000)
19. H.M. Osinga, J. Rankin, Two-parameter locus of boundary crisis: mind the gaps, in *Proceedings of The 8th AIMS International Conference, 2010*, edited by W. Feng, Z. Feng, M. Grasselli, A. Ibragimov, X. Lu, Stefan Siegmund, J. Voigt (American Institue of Mathematical Sciences, 2011), pp. 1148–1157
20. J. Palis, F. Takens, *Hyperbolicity & Sensitive Chaotic Dynamics at Homoclinic Bifurcations* (Cambridge University Press, 1993)
21. E. Pugliese, R. Meucci, S. Euzzor, J.G. Freire, J.A. Gallas, Complex dynamics of a dc glow discharge tube: Experimental modeling and stability diagrams, Sci. Rep. **5**, 8447 (2015)
22. S. Serrano, R. Barrio, A. Dena, M. Rodríguez, Crisis curves in nonlinear business cycles, Comm. Nonl. Sci. Numer. Sim. **17**, 788 (2012)
23. C. Simó, On the Hénon-Pomeau attractor, J. Stat. Phys. **21**, 465 (1979)
24. E. Sander, J.A. Yorke, Period-doubling cascades galore, Ergodic Th. Dynam. Sys. **31**, 1249 (2011)
25. E. Sander, J.A. Yorke, Connecting period-doubling cascades to chaos, Int. J. Bifurc. Chaos **22**, 1250022 (2012)
26. M.D. Shrimali, A. Prasad, R. Ramaswamy, U. Feudel, Basin bifurcations in quasiperiodically forced coupled systems, Phys. Rev. E **72**, 036215 (2005)
27. Y. Ueda, Randomly transitional phenomena in the system governed by Duffing's equation, J. Stat. Phys. **20**, 181 (1979)
28. Y. Ueda, Explosion of strange attractors exhibited by Duffing's equations, Ann. Acad. Sci. **357**, 422 (1980)
29. A. Witt, U. Feudel, A. Pikovsky, Birth of strange nonchaotic attractors due to interior crisis, Physica D **109**, 180 (1997)